Applied Thermal Engineering 114 (2017) 1498–1506

Contents lists available at ScienceDirect

Applied Thermal Engineering

journal homepage: www.elsevier.com/locate/apthermeng

Research Paper

Robust multi-objective control of hybrid renewable microgeneration systems with energy storage

John Allison

Energy Systems Research Unit, Department of Mechanical & Aerospace Engineering, University of Strathclyde, James Weir Building, 75 Montrose Street, Glasgow G1 1XJ, United Kingdom

HIGHLIGHTS

- A hybrid energy system of micro-CHP, solar PV, and battery storage is presented.
- Possible to exploit synergy of systems to fulfil the thermal and electrical demands.
- Can control to minimise the interaction with the local electrical network.
- Three different control approaches were compared.
- The nonlinear inversion-based control strategy exhibits optimum performance.

ARTICLE INFO

Article history:
Received 8 April 2016
Revised 4 July 2016
Accepted 13 September 2016
Available online 14 September 2016

Keywords:
Microgeneration
Multi-objective control
Hybrid renewable energy systems
Simulation
Feedback linearisation
Robust control

ABSTRACT

Microgeneration technologies are positioned to address future building energy efficiency requirements and facilitate the integration of renewables into buildings to ensure a sustainable, energy-secure future. This paper explores the development of a robust multi-input multi-output (MIMO) controller applicable to the control of hybrid renewable microgeneration systems with the objective of minimising the electrical grid utilisation of a building while fulfilling the thermal demands. The controller employs the inverse dynamics of the building, servicing systems, and energy storage with a robust control methodology. These inverse dynamics provides the control system with knowledge of the complex cause and effect relationships between the system, the controlled inputs, and the external disturbances, while an outer-loop control ensures robust, stable control in the presence of modelling deficiencies/uncertainty and unknown disturbances. Variable structure control compensates for the physical limitations of the systems whereby the control strategy employed switches depending on the current utilisation and availability of the energy supplies. Preliminary results presented for a system consisting of a micro-CHP unit, solar PV, and battery storage indicate that the control strategy is effective in minimising the interaction with the local electrical network and maximising the utilisation of the available renewable energy.

1. Introduction

Microgeneration technologies (MGTs) are positioned to address future building energy efficiency requirements and facilitate the integration of renewables into buildings to ensure a sustainable, energy-secure future. Microgeneration technology provides energy production in the building for the building, which can considerably improve the current model of centralised power stations servicing national-scale electrical grids.

Microgeneration is frequently coupled with energy storage and collectively known as 'distributed resources'. This technology pairing permits control of intermittent renewable resources by storing generated energy and then dispatching it from the storage when called upon from energy demands of the building. The intermittent electrical-power-generating MGTs (micro-wind, micro-hydro, solar photovoltaics (PV)) particularly benefit from being deployed in tandem with electrical energy storage (EES) as there is usually a mismatch between power generation demand and supply.

The building's connection to the local electrical grid is the prevalent 'solution' to the mismatch between the electrical power generation in the building and the electrical loads. When the combined utility of EES, dispatchable electrical-power generating microgeneration, and renewable resources cannot fulfil the electrical requirements of the building, the building will import electrical power from the local network. Conversely, when there is an excess generation from all sources, the building will export the surplus to

E-mail address: j.allison@strath.ac.uk

http://dx.doi.org/10.1016/j.applthermaleng.2016.09.070
1359-4311/

Nomenclature

$\dot{m}_{\text{fuel}}$	fuel flow rate supply to CHP unit
η_e	electrical efficiency of CHP unit
η_t	thermal efficiency of CHP unit
$\overline{LHV}$	lower heating value of fuel supply
$\boldsymbol{P}$	system inertia compensator
$\boldsymbol{Q}$	decoupling matrix
Φ_{sol}	solar heat gain
ρ	relative degree of input-output system
$\Theta_{\text{rad},i}$	temperature of radiator node i
$\Theta_{\text{s},i}$	temperature of structural component i
Θ_{a}	temperature of air
Θ_{cw}	temperature of cooling water
Θ_{eng}	temperature of engine block
$\boldsymbol{r}$	integrator state
$\boldsymbol{u}$	controlled input vector
$\boldsymbol{v}$	synthetic input vector
$\boldsymbol{x}$	state vector
$\boldsymbol{y}$	output vector
C_{a}	heat capacity of air
C_{cw}	heat capacity of cooling water
C_{eng}	heat capacity of engine block
C_{rad}	heat capacity of radiator
C_{s}	heat capacity of structural component
e	error signal
G	transfer function
K	controller gain
m	number of measured outputs and controlled inputs
n	model order (number of state-variables)
w	exogenous signal

the local network. However, remote communities or small islanded commercial premises may not have access to a local electrical network or be willing to pay for new infrastructure to connect to central generation stations [1]. Even when a connection to the grid is possible, a high penetration of intermittent renewable energy in the electrical grid and the buildings themselves will result in a reduction of the current network's ability to absorb excess generation freely or be able to always supply energy when the building requires.

Fortunately, there is potential to exploit the synergy between some of the MGTs that can work together to fulfil the thermal and electrical demands of the building to alleviate the reliance on the local electrical network. The emerging technology combination is that of micro-combined heat and power (CHP) and solar PV, shorted to combined heat and photovoltaics (CHPV). The harmony between the technologies is greatest in colder climates where the micro-CHP units' maximum output is during winter when the thermal demands of the building are high while the solar PV generation is at its lowest; with the opposite scenario observed in the summer months. Combining this system with EES that can regulate the mismatch in generation (which could be small were the systems sized appropriately), then it could offer complete independence from the electrical network. However, matching the dynamic availability of PV systems with the power generation from a CHP engine can be challenging and will require intelligent control algorithms that are aware of the interaction the technologies have with both the thermal and electrical networks within the building.

Many of the current approaches to the control of these hybrid energy supply systems involve model predictive control (MPC) [2,3], and/or optimisation methods [4,5]. These are very useful tools for determining the feasibility of a proposed energy supply system or the optimal operational strategy over a future time horizon, provided the assumptions on the performance of the systems be in line with those predicted by the models. However, the issue with these approaches is that they not only rely on accurate models to predict the optimum operation regime but rarely is attention given to the control strategy used while in operation. It assumes that a thermally-led CHP unit is capable of providing the thermal load when it is required, and similarly for electrically-led systems [6, p. 43].

The objective of optimal or MPC control strategies for microgeneration typically concerns minimising cost or maximising profit [7, Section 3.1], with a secondary concern for operational constraints. With a limited or non-existent grid connection, emphasis should be placed on the security of the energy supply within the building.

Another complication with the existing strategies is that energy systems – and the external environment in which they operate – cannot be modelled precisely, may change in an unpredictable manner, and may be subject to significant disturbances. The design of energy management systems in the presence of significant uncertainty requires the development of robust control algorithms. This research explores the development of multi-input multi-output (MIMO) control algorithms and their application to the problem of controlling microgeneration devices and energy storage within a building with the primary objectives of fulfilling the thermal and electrical demands of the building while minimising the interaction with the local electrical network.

2. Control theory

The controller combines the inverse dynamics of the building, servicing systems, and energy storage with a robust control methodology. These inverse dynamics provides the controller with knowledge of the complex cause and effect relationships between the system, the controlled inputs, and the external disturbances, while an outer-loop control ensures robust, stable control in the presence of modelling deficiencies/uncertainty and unknown disturbances. Variable structure control compensates for the physical limitations of the systems whereby the control strategy employed switches depending on the current utilisation and availability of the energy supplies.

A robust control method allows the models to be imprecise, where the imprecision in this system stems from two major areas:

System uncertainty: It is not possible to know precisely the system parameters (e.g. the exact heat capacity of the building structure, or the heat transfer coefficients, the operational efficiency, or the vast array of disturbances to the system).

Simplified dynamics: The models used in systems-level studies are a *purposefully* simplified representation of the physical systems (e.g. using a reduced model of the building structure, modelling the radiation heat transfer as linear, neglecting the modelling of the high frequency dynamical modes, such as internal components of the CHP plant or thermal store).

In control literature, these two areas of imprecision are known as **structured** uncertainties (related to the parametric uncertainties) and **unstructured** uncertainties (the unmodelled or reduced-order dynamics) [8].

Robust controllers are comprised of two parts:

1. The inner model reduction component – commonly a feedback linearisation or inverse control law, and

2. an outer component used to account for the uncertainties.

The following sections details these two components of the controller that can be used for the robust control of hybrid renewable energy systems in buildings.

2.1. Nonlinear inversion control law

The theoretical basis for the control approach in this section is based on the work of Cheng et al. [9] and is known as input-output feedback linearisation, which has been successfully applied in related fields of large-scale power systems [10], solar collector fields [11], and air handling units [12]. The design procedure is briefly outlined here with more detailed description of the theory available elsewhere [13–15].

The differential equations that govern the dynamics of the building, building services and its energy systems can be written in state-space form as the class of nonlinear MIMO control/input-affine systems described by

$$\begin{aligned}\dot{\boldsymbol{x}}(t) &= \boldsymbol{f}(\boldsymbol{x}(t)) + \boldsymbol{G}(\boldsymbol{x}(t))\boldsymbol{u}(t)\\ \boldsymbol{y}(t) &= \boldsymbol{h}(\boldsymbol{x}(t))\end{aligned} \tag{1}$$

where $\boldsymbol{x}(t) \in \mathbb{R}^n$ is the state vector, $\boldsymbol{y}(t) \in \mathbb{R}^m$ are the measured outputs, $\boldsymbol{u}(t) \subset U \in \mathbb{R}^m$, are the controlled inputs, $\boldsymbol{f} : \mathbb{R}^n \to \mathbb{R}^n$ and $\boldsymbol{h} : \mathbb{R}^n \to \mathbb{R}^m$ are smooth vector fields, and $\boldsymbol{G} : \mathbb{R}^n \to \mathbb{R}^n \times \mathbb{R}^m$ is a matrix whose columns $\boldsymbol{g}_j : \mathbb{R}^n \to \mathbb{R}^n, j = 1, \ldots, m$ are smooth vector fields. Also, for notational compactness from now on the time-dependence is implied so that $\boldsymbol{x} := \boldsymbol{x}(t), \boldsymbol{u} := \boldsymbol{u}(t), \boldsymbol{y} := \boldsymbol{y}(t)$.

The control objective is to make any output y_i (such as internal air temperature, or electrical grid power use) track a desired trajectory while keeping the system stable. The difficulty with this is that any output is only indirectly related to a controlled input, through the state variables and the nonlinear state equations. For example, a direct convective air heater will have a more deliberate effect on the air temperature that a hydronic radiator. The inability to quickly see a change in the output based upon a change in the controlled input often results in poor control and inefficient utilisation of the energy systems. In buildings a common result of this is overheating/cooling.

A measure of this 'indirectness' is called the relative order/degree of the output. From the mathematical representation of the system (1), it is possible to calculate the relative degree of each output in relation to the controlled inputs. This is determined by continually differentiating the output of the system until the control appears:

$$\dot{y}_i = \frac{\mathrm{d}h_i(\boldsymbol{x})}{\mathrm{d}t} = \frac{\partial h_i(\boldsymbol{x})}{\partial \boldsymbol{x}}\frac{\mathrm{d}\boldsymbol{x}}{\mathrm{d}t} = \mathcal{L}_{\boldsymbol{f}} h_i(\boldsymbol{x})$$

$$\ddot{y}_i = \frac{\partial \mathcal{L}_{\boldsymbol{f}} h_i(\boldsymbol{x})}{\partial \boldsymbol{x}}\frac{\mathrm{d}\boldsymbol{x}}{\mathrm{d}t} = \mathcal{L}_{\boldsymbol{f}}^2 h_i(\boldsymbol{x})$$

$$\vdots$$

$$y_i^{(k)} = \mathcal{L}_{\boldsymbol{f}}^k h_i(\boldsymbol{x}), \quad \text{for } k < \rho_i$$

$$y_i^{(\rho_i)} = \mathcal{L}_{\boldsymbol{f}}^{\rho_i} h_i(\boldsymbol{x}) + \sum_{j=1}^{m} \mathcal{L}_{\boldsymbol{g}_j}\mathcal{L}_{\boldsymbol{f}}^{\rho_i - 1} h_i(\boldsymbol{x}) u_j$$

where $\mathcal{L}$ denotes the Lie derivative, and for at least one j-th input, $\mathcal{L}_{\boldsymbol{g}_j}\mathcal{L}_{\boldsymbol{f}}^{\rho_i - 1} h_i(\boldsymbol{x}) \neq 0$, and ρ_i denotes the relative degree of output y_i i.e. the relative degree corresponds to the lowest order derivative of the output that depends explicitly on an input.

The same method can be applied to each output of the system (1) and written together in a single compact vector-matrix equation as

$$\underbrace{\begin{bmatrix} y_1^{(\rho_1)} \\ y_2^{(\rho_2)} \\ \vdots \\ y_m^{(\rho_m)} \end{bmatrix}}_{\dot{\boldsymbol{y}}} = \underbrace{\begin{bmatrix} \mathcal{L}_{\boldsymbol{f}}^{\rho_1} h_1(\boldsymbol{x}) \\ \mathcal{L}_{\boldsymbol{f}}^{\rho_2} h_2(\boldsymbol{x}) \\ \vdots \\ \mathcal{L}_{\boldsymbol{f}}^{\rho_m} h_m(\boldsymbol{x}) \end{bmatrix}}_{\boldsymbol{P}(\boldsymbol{x})} + \underbrace{\begin{bmatrix} \mathcal{L}_{\boldsymbol{g}_1}\mathcal{L}_{\boldsymbol{f}}^{\rho_1 - 1} h_1(\boldsymbol{x}) & \ldots & \mathcal{L}_{\boldsymbol{g}_m}\mathcal{L}_{\boldsymbol{f}}^{\rho_1 - 1} h_1(\boldsymbol{x}) \\ \mathcal{L}_{\boldsymbol{g}_1}\mathcal{L}_{\boldsymbol{f}}^{\rho_2 - 1} h_2(\boldsymbol{x}) & \ldots & \mathcal{L}_{\boldsymbol{g}_m}\mathcal{L}_{\boldsymbol{f}}^{\rho_2 - 1} h_2(\boldsymbol{x}) \\ \vdots & \ldots & \vdots \\ \mathcal{L}_{\boldsymbol{g}_1}\mathcal{L}_{\boldsymbol{f}}^{\rho_m - 1} h_m(\boldsymbol{x}) & \ldots & \mathcal{L}_{\boldsymbol{g}_m}\mathcal{L}_{\boldsymbol{f}}^{\rho_m - 1} h_m(\boldsymbol{x}) \end{bmatrix}}_{\boldsymbol{Q}(\boldsymbol{x})} \boldsymbol{u}$$

or

$$\hat{\boldsymbol{y}} = \boldsymbol{P}(\boldsymbol{x}) + \boldsymbol{Q}(\boldsymbol{x})\boldsymbol{u}$$

If the matrix $\boldsymbol{Q}(\boldsymbol{x})$ is invertible, then utilising feedback control of the form

$$\boldsymbol{u} = (\boldsymbol{Q}(\boldsymbol{x}))^{-1}(-\boldsymbol{P}(\boldsymbol{x}) + \boldsymbol{v}) \tag{2}$$

results in the simple linear system $\left(y_1^{(\rho_1)} = v_1, \ldots, y_m^{(\rho_m)} = v_m\right)$, where each v_i is an outer-loop control law to be defined in order to achieve the required performance tracking on y_i. It can be seen that utilising (2) has resulted in an input-output relation that is linearised *and* decoupled, such that each output y_i is a linear function of a single input v_i.

2.2. Robust outer-loop control

To achieve robust control v_i that is designed so that the output y_i asymptotically tracks the demand trajectory $y_{\mathrm{d},i}$. For example, in building and energy systems control, demand trajectories are typically the air temperature set-points. For this work, an outer-loop controller has been utilised that is a combination of local asymptotic stabilisation (via pole placement) and integral action. This type of control, known as pseudo-derivative-feedback (PDF) control, was pioneered by Phelan [16] as an alternative to the traditional proportional-integral (PI) controller that is used in most of cases in the industry. This control has been proven to perform better than PI for systems with $\rho_i \leqslant 2$) [16, Appx. C], but is also applicable to systems $\rho_i > 2$. The superior performance is gained by not introducing zeros into the system allowing for a faster transient response with less overshoot.

The generalised PDF control is given by

$$v_i = r_i - \sum_{q=1}^{\rho_i} K_{\mathrm{d},q} y_i^{(q-1)}, \quad i = 1, \ldots, m \tag{3}$$

where $\dot{r}_i = K_{\mathrm{I},i}(y_{\mathrm{d},i} - y_i) = K_{\mathrm{I},i} e_i$ and $\boldsymbol{k}_i = (K_{\mathrm{I},i}, K_{\mathrm{d},1}, \ldots, K_{\mathrm{d},\rho_i})$ are the controller gains. System performance can then be tuned via any pole-placement technique by manipulating the controller gains $\boldsymbol{k}_i$ to get the required tracking performance.

2.3. Input constraints

The performance of all real systems is limited by the capabilities of the actuators that are responsible for the transfer of energy from the control system to the process being controlled. The actuating control value that supplies fuel to the CHP engine has a maximum and minimum fuel supply, as well as restricted rate at which the fuel can be delivered. Electrical energy storage also has low-level electronics that restricts the maximum permissible current that can be transferred to the device to avoid overheating and to protect their inner circuitry. Many of these discontinuous limits are designed to ensure safe performance of the energy system, and so the 'high-level' controller should be respectful of these system limitations to ensure optimal and safe control.

There are many cases when a system may reach the limits of the actuator; this can be when there is a large change in set-point such that the system must drive as hard as possible to reach its target.

There is also the case where a large disturbance may cause the actuator to saturate. A well-designed controller should be capable of handling *exceptional* disturbances, i.e. disturbances of intensity higher than the predicted bounds which are used when tuning the control parameters. If integral control is used in such cases, the integral term in the control action may become unreasonably large, so that once the disturbance stops, the system goes through large amplitude oscillations in order to return to the desired trajectory, this is commonly known as integrator wind-up.

The most effective way to cope with integrator wind-up is to design a variable structure controller so that when the controller output has reached either limit, any future control action must either keep u_i constant or reduce it so that it will continue its normal linear mode of operation [17]. To implement this new switching surface with a PDF controller, first define the following nonlinear piecewise 'dead zone' function, where for an given input u_i, the output $\tilde{u}_i$ is given by

$$\tilde{u}_i = \begin{cases} 0 & \text{if } u_{\min,i} \leqslant u \leqslant u_{\max,i} \\ u_i - u_{\max,i} & \text{if } u_i > u_{\max,i} \\ u_i - u_{\min,i} & \text{if } u_i < u_{\min,i} \end{cases}$$

When $\tilde{u}_i \neq 0$ then the system has been overdriven as the controller output, u_i, is out of the physical limits $(u_{\min,i}, u_{\max,i})$. This can be represented as the logical function $b_{\text{sat}} := \tilde{u}_i \neq 0$.

In addition, if the error signal would cause the system to move further into the saturation region then the integrator should be clamped. This is determined by sign of the error, $\text{sgn}(e_i)$. When it is the same as $\tilde{u}_i$ then the system will be pushed further into the saturation region. This is represented by the logical function: $b_{\text{inc}} := e_i \cdot \tilde{u}_i > 0$.

The new integrator clamping logic is implemented as

$$\dot{r}_i = \begin{cases} 0 & \text{if } b_{\text{sat}} \wedge b_{\text{inc}} \\ K_{\text{I},i} e_i & \text{otherwise} \end{cases} \tag{4}$$

The synthesis of the nonlinear variable structure inversion control law (2), the outer-loop PDF control (3), and input constraint compensation (4) is given in the block diagram schematic of Fig. 1.

2.4. Variable structure control

The control law (2) and (3) will provide decoupled system performance for each output provided the computed inputs do not violate the constraints, while the compensation scheme (4) will prevent unstable behaviour of the controller were the control to reach any of these limits. However, the computed control action of one input may be dependent on the control action of another. In this work, the inversion control law (2) is re-designed to account automatically for this coupling of control channels. Therefore, the controller must dynamically update the structure of the inversion component (2) when any constraint is reached otherwise one of the control inputs will be computed based on the expected control input from the other channel. Were it not to be updated a constrained input on one channel will result in the other control channels not adequately accounting for the restricted value of the other input.

3. Case study

What follows is an example application of the theory to a small office zone that has a hybrid energy supply system of micro-CHP, solar PV, and electrical energy storage.

The zone modelled is a small office located in Trappes, France, for which the climatic data is available. Fig. 2 shows the wire-frame drawing of a single office zone, with major dimensions indicated. The overall office controlled consists of four of these zones in parallel, joined along their length so that all windows are facing west. The thermal demands of the zone are served by a hydronic radiator system supplied by a Stirling-engine based CHP system. The electrical demands are fulfilled by the electrical generation of the CHP, PV, and electrical energy storage. The chosen control objective is to make the measured air temperature track a desired trajectory while minimising the electrical grid utilisation. The difficulty is that the air temperature is only indirectly related to the input fuel flow rate – which must first influence the engine, cooling water, and radiator temperatures before changes to the internal air temperature will be seen. The number of 'elements' or states downstream of the control input represent the relative order/degree of that output. It is not straightforward to see how the input can be designed to control the tracking behaviour of the output.

3.1. System specifications

The CHP specifications are based upon a WhisperGEN CHP engine, with empirical data taken from [18] (see Table 1). The engine has an external pump, and a permissible water flow rate of 31–81 min^{-1}. This particular engine has a small electrical capacity of 750 W (nominal) – equivalent to 575 W once the parasitic electrical consumption of the CHP is subtracted – and large

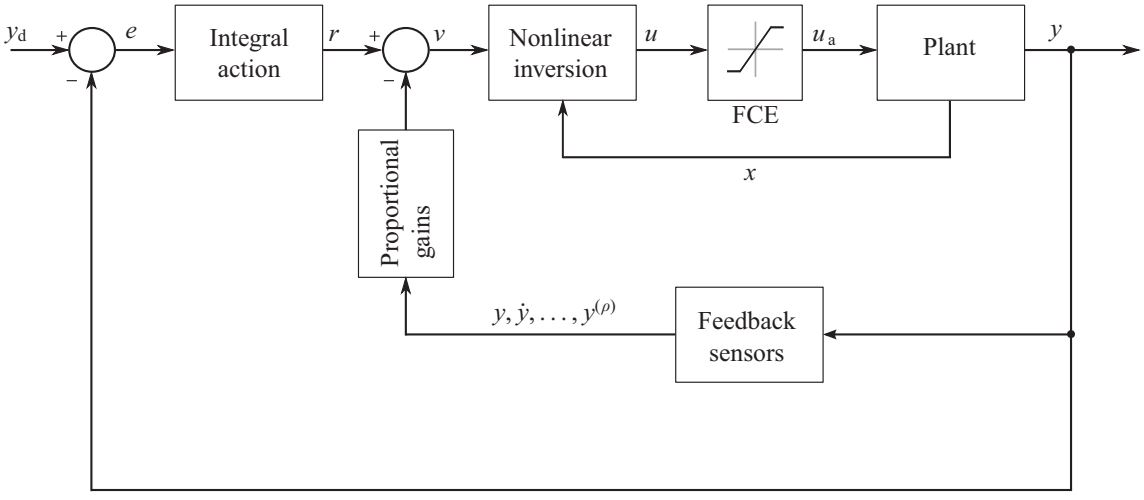

Fig. 1. Schematic of control theory.

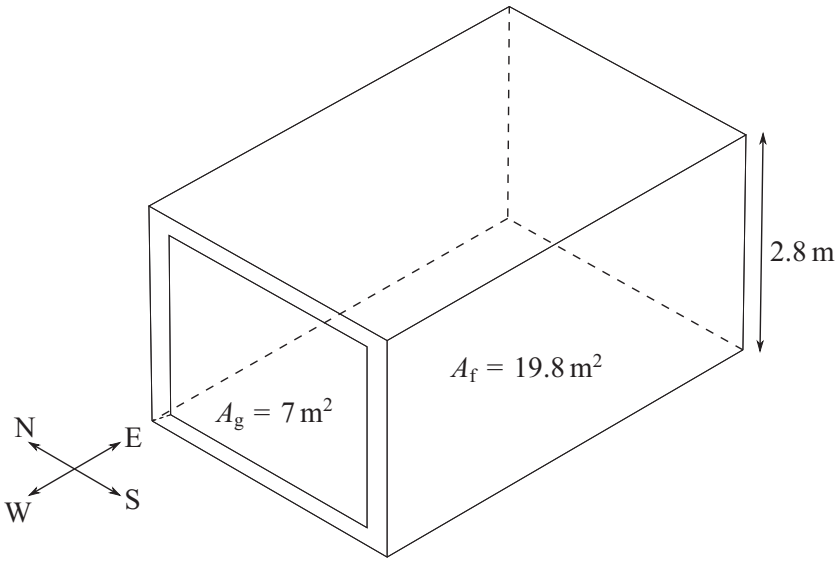

Fig. 2. Wire frame drawing of building zone modelled.

Table 1
Model parameters for case study.

Cogeneration device		Fuel composition		Hydronic system		Building zone	
C_{eng}	18.5×10^3 J K^{-1}	H_2	0.00%	c_p	4192 J kg^{-1} K	I_{load}	20 W m^{-2}
C_{cw}	28.1×10^3 J K^{-1}	CH_4	94.76%	$\dot{m}_{cw}$	0.2 kg s^{-1}	f_{int}	0.5
H_{HX}	31.8 W K^{-1}	C_2H_6	2.70%				
H_{loss}	4.64 W K^{-1}	C_3H_8	0.23%				
η_e	0.0929	N_2	1.76%				
η_q	0.970	CO_2	0.55%				
		$\overline{LHV}$	35.16 MJ m^{-3}				

Controller

$\boldsymbol{k}_1 = (349.36 \times 10^{-12}, 321.46 \times 10^{-9}, 90.69 \times 10^{-6}, 6.03 \times 10^{-3}, 137.78 \times 10^{-3})$
$\boldsymbol{k}_2 = (71.11 \times 10^{-3}, 533.33 \times 10^{-3})$
$\boldsymbol{x}(0) = (6.01, 5.68, 5.68, 5.66, 4.84, 4.84, 0)^\top, \boldsymbol{r}(0) = (0, 0)^\top$

thermal output 6.5 kW (nominal). The typical application is residential micro CHP, but is shown here to be applicable to an array of small office zones. These engines are typically controlled by heat demand (heat-led) rather than electrical demand. The control developed here is 'led-agnostic', as the CHP is operated based upon the prevailing demands of both the thermal and electrical networks due to the decoupling control law.

The unit also has several low-level controls: the unit will shutdown if the cooling water temperature at the outlet of the system exceeds 85 °C. The cool-down period of the unit was 25 min, but is assumed that the cool-down period is *optional*, that is if the unit receives demand while in cool-down mode it will switch to warm-up before completing the entire cool-down period. For the purpose of control demonstration, it is assumed that the unit can also modulate down to as low as 3 kW, while still generating electricity. Furthermore, a fixed efficiency and heat-to-power ratio is also assumed.

The results given here are calculated using two reference inputs. This heating set-point is 20 °C between 08:00 and 18:00 on weekdays, with a night time and weekend setback temperature of 12 °C. The electrical grid power set-point is set to zero. This means that the controller will strive to neither import or export from or to the national grid, thereby minimising the interaction with the local electrical network.

The electrical loads are comprised of the internal gains, at 20 W m^{-2}, which equates to a standing load of 396 W for each cell between 08:00 and 18:00 during weekdays. The energy production from photovoltaics is calculated using PVWatts [19]. The PV system characteristics consist of a 650 W solar array, south facing with a fixed tilt of 48.73° (which is equal to the latitude of the climate data).

3.2. Electrical grid measurement

The theoretical electrical grid use is based upon an energy balance with all demand and supply elements given by:

$$y_2 = P_{grid} = P_{load} - P_{bat} - P_{PV} - P_{CHP} \tag{5}$$

It can be seen from (5) that the availability of PV is considered a disturbance. In this way, priority is given to utilising as much of the PV-generated electricity as possible, while the combined efforts of the CHP unit and battery storage can compensate for the remaining demand.

However, note that in (5) the control is immediately affecting the output of the system i.e. the electrical grid output has a relative degree of zero, that is, the manipulated fuel flow rate and battery (dis/)charge instruction has an immediate and direct effect on the interaction with the electrical grid.

To apply the theory in such situations, an output-redefinition method is used. Provided that the new output function is defined in such a way that it is essentially the same as the original output function in the frequency range of interest, exact tracking of the

new output function then also implies good tracking of the original output y_i. i.e. the electrical grid regulation will still be achieved since the outer-loop compensator will drive the actual output to zero.

The output-redefinition method is achieved by introducing an additional state for the electrical grid power, given by

$$\dot{\widehat{P}}_{\text{grid}} = 1/\tau_{\text{grid}}(P_{\text{grid}} - \widehat{P}_{\text{grid}}) \tag{6}$$

This increases the relative order of the electrical grid output by one, so that (2) can be implemented directly. The time constant τ_{grid} dictates how quickly the control model will estimate the actual grid use.

3.3. Plant models

There are a number of Stirling-engine based dynamic CHP models in the literature [20–22] but the Annex 42 model [23] was selected for this work as it was the simplest model that was still independently empirically validated [24]. Original validation of the model was carried out in [25]. The engine model consists of three control volumes (subsystems): (1) Energy conversion, (2) engine, (3) cooling water. The subsystem models used for the controller are provided in Appendix A.

3.4. Building model

The building model utilised by the controller is a simplified dynamic building model with energy performance results validated [26] with European Standard EN 15265 [27]. Each enclosure component (e.g. wall, floor, ceiling) are assigned two thermodynamic temperature nodes according to the theory of [28], which can account for the fluctuations seen on either side of a construction in typical residential and office zones.

The overall system to be controlled can be expressed in a general state-space form by combining the zone equations and plant models and selecting the state vector as $\boldsymbol{x} = (\Theta_{\text{eng}}, \Theta_{\text{cw}}, \Theta_{\text{rad,1}}, \Theta_{\text{rad,2}}, \Theta_{\text{a}}, \Theta_{\text{s}})^{\top}$ and the control inputs $\boldsymbol{u} = (\dot{m}_{\text{fuel}}, P_{\text{bat}})^{\top}$, the measured exogenous signals as $\boldsymbol{w} = (P_{\text{load}}, P_{\text{pv}})^{\top}$, disturbances as $\boldsymbol{d} = (\Theta_{\text{e}}, \Phi_{\text{sol}})^{\top}$ and system outputs $\boldsymbol{y} = (\Theta_{\text{a}}, P_{\text{grid}})^{\top}$.

The inversion control-law does not assume knowledge of any of the disturbance signals to the model, these are compensated for by the outer-loop control. Increased control performance could be attained by incorporating an estimate of the disturbances, such as the rate of heat loss to the outside environment.

Furthermore, the modelling inaccuracies are addressed by the use of the outer-loop PDF control, which compensates for the matched disturbances and parameter inaccuracies. For hybrid energy supply systems with highly nonlinear behaviour or a wide range of required operation the control law (2) will provide the best performance but at additional computational expense.

3.5. Simulation results

Figs. 3–9 show the dynamic results from the model for a cold, bright day. The sampling frequency of the controller was set to 1 Hz with an output frequency of 3.33 mHz. Best performance and accurate simulation from the numerical solver is achieved when the update period of the controller is set four to five times faster than the slowest time constant in the system.

As can be seen in Figs. 3 and 4, the nonlinear inversion plus PDF (NI + PDF) control is able, after a stable transient period, to maintain the set-point temperature with no oscillation or 'ringing' around the set-point typically associated with thermally-led CHP switching on and off to fulfil the demand. In addition to the On/Off control, the performance of a conventional PD control tuned

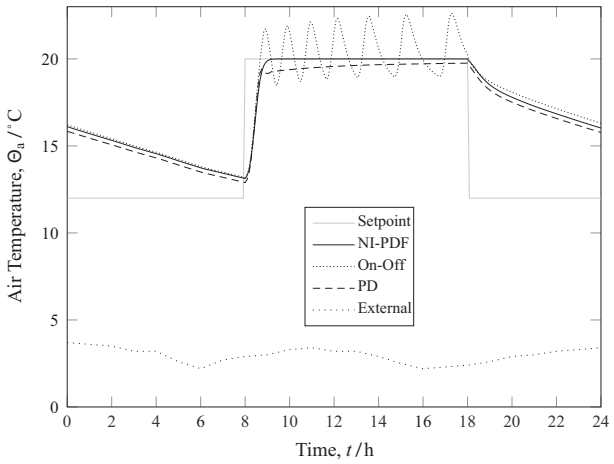

Fig. 3. Comparison of dynamic response of air temperature over 24 h period.

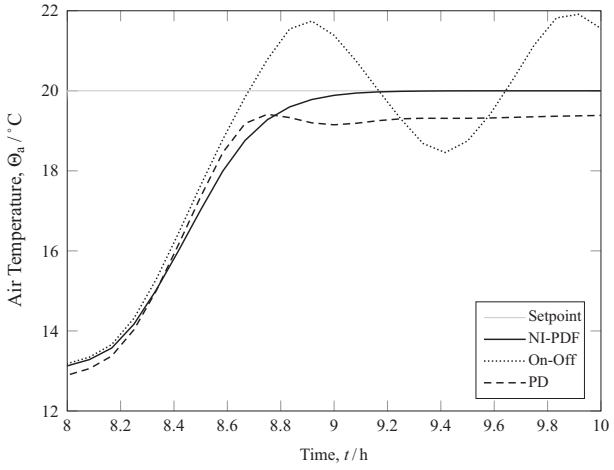

Fig. 4. Comparison of dynamic response of air temperature during transient period for a positive setpoint change at the beginning of the occupied duration.

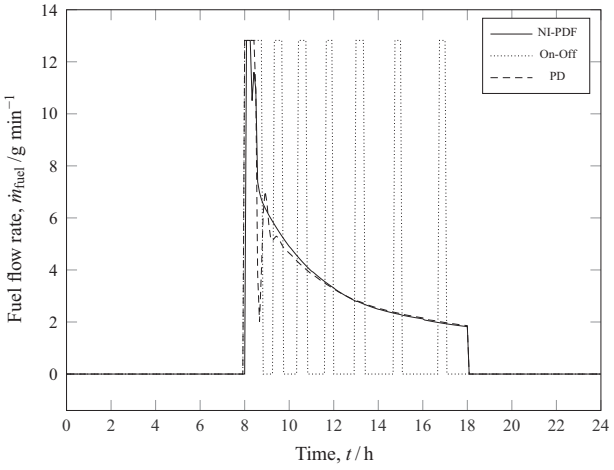

Fig. 5. Comparison of manipulated fuel flow rate over 24 h period.

with Simulink's Control System Design toolbox has been presented alongside for comparison.

The PD control undershoots the set-point and takes a long time to converge towards the set-point temperature and is unable to

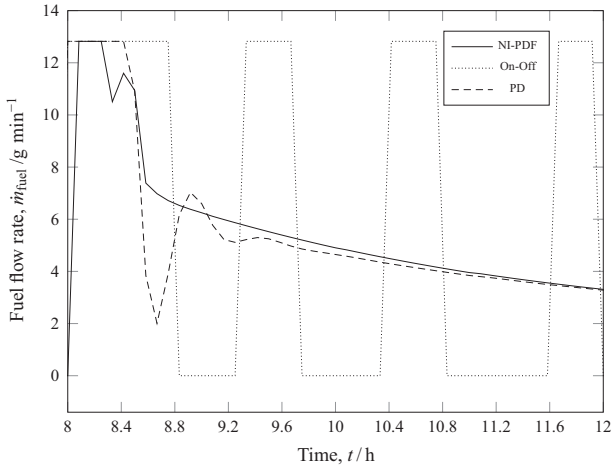

Fig. 6. Comparison of manipulated fuel flow rate during transient period for a positive setpoint change at the beginning of the occupied duration.

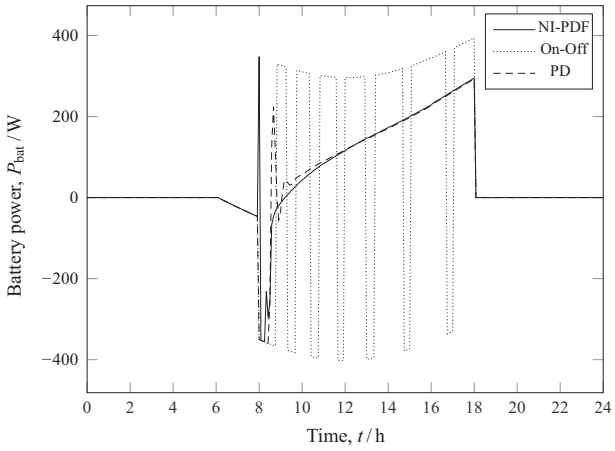

Fig. 7. Comparison of manipulated battery power over 24 h period.

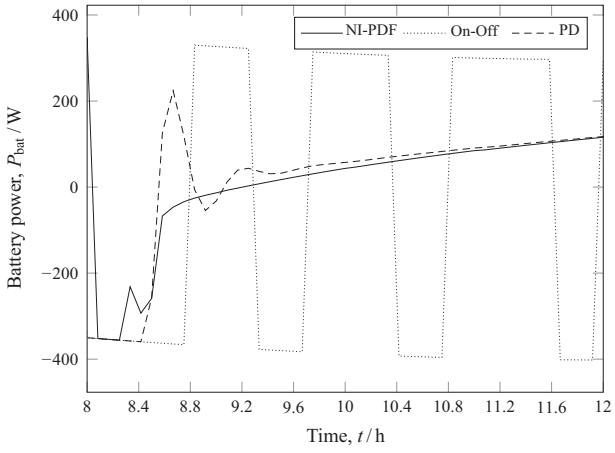

Fig. 8. Comparison of manipulated battery power during transient period for a positive setpoint change at the beginning of the occupied duration.

reach the set-point within the occupied term. The PD control also demonstrates large fluctuations in control action on the manipulated fuel flow rate during the start-up period (see Fig. 6), while the NI + PDF controller holds the fuel flow rate at maximum before

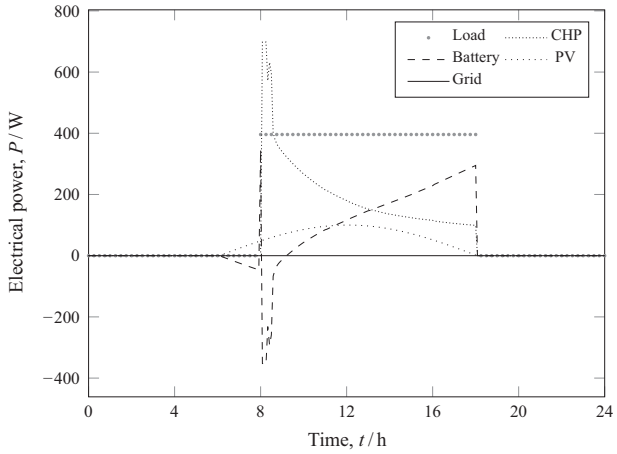

Fig. 9. Comparison of all electrical power interactions over 24 h period.

safely decreasing the fuel input to the minimum permissible value before the valve is closed.

The control of the air-temperature response time was selected to settle within 2% of the set-point after 30 min with no overshoot. However, the CHP unit is not sufficiently sized to achieve the desired performance and saturates at its maximum output. This leads to a slower response (settling after $\approx$ 1 h) but the controller still achieves the set-point temperature with no threat of overshoot or oscillatory response due to the input constraint compensation. While the air temperature demonstrated a slower response than for which it was tuned, if the controller were to be re-tuned for a faster response time, all that would be shown is the fuel flow input spending a longer amount of time at its saturation limit before safely moving away from the limit until the desired temperature is reached.

Fig. 9 shows all of the elements of the electrical network working together to achieve zero electrical grid interaction. This demonstrates the strength of the robust control strategy as it is able to balance both the thermal and electrical networks without any reliance upon the electrical grid.

It can be seen that the balance of power extracted and supplied to the battery will leave it in a more discharged state at the end compared to its initial state. However, there will be other days where the excess generation from the PV and CHP would leave the battery in a surplus. Nonetheless, were the battery to be completely depleted the following results can be surmised: the control strategy here only has two manipulable inputs (CHP fuel flow rate and battery use). When the battery is depleted, the system loses a controllable input. In this case the control law would be dynamically recomputed to a single-input single-output (SISO) system (see Section 2.4). It is up to the control engineer to decide whether to control the CHP to meet the thermal or electrical demand. With no back up thermal heating system, it would control to fulfil the thermal demands and make up the deficit in power generation from the grid.

4. Conclusion

A robust nonlinear control strategy has been presented, with potential application to a vast array of hybrid energy supply systems that have coupled electrical and thermal demands. The control can fulfil the thermal demands of the building while facilitating flexible interaction with the local electrical network.

The control is a pragmatic solution that runs in real-time without knowledge of the external environment or future prediction of zone use or availability of energy sources. It is also respectful of

undersized heating systems and actuating elements so that the system remains stable and achieves best possible performance in the face of parameter uncertainty and modelling inaccuracies.

Only preliminary dynamic simulation results have been presented here, as the emphasis was placed on the underlying theory and its application to general energy systems. The case shown here is a limited one with only two controllable inputs, however, it is expected the strength of this control strategy will be when there are many more that can affect both the thermal and electrical demands. Future work will detail its application to larger and more in-depth case studies, and to demonstrate its performance at yearly resolution in comparison to existing control methods. After which the real-world performance analysis of the controller will be tested by embedding the controller in hardware/software and examining the performance of a prototype of the system. It is thought that the robust controller design may accommodate for the difference in performance seen in real-world deployments versus that recorded in laboratory/simulations conditions.

Acknowledgements

This research was funded in partnership with a BRE Trust grant as part of the University of Strathclyde's BRE Centre of Excellence in Energy Utilisation and with an EPSRC research grant (EP/P505747/1).

Appendix A. Systems-level models for controller

A.1. Cogeneration model

CHP engine performance correlation:

$$\Phi_{\text{gross}} = \overline{LHV}\dot{m}_{\text{fuel}}$$
$$P_{\text{chp}} = \eta_{\text{e}}\Phi_{\text{gross}}$$
$$\Phi_{\text{gen}} = \eta_{\text{t}}\Phi_{\text{gross}}$$

Engine control volume:

$$C_{\text{eng}}\dot{\Theta}_{\text{eng}} = \Phi_{\text{gen}} - \Phi_{\text{HX}} \tag{A.1}$$

Cooling water heat exchanger control volume:

$$C_{\text{cw}}\dot{\Theta}_{\text{cw}} = (\dot{m}c_p)_{\text{cw}}(\Theta_{\text{rad},2} - \Theta_{\text{cw}}) + \Phi_{\text{HX}} \tag{A.2}$$

where $\Phi_{\text{HX}} = H_{\text{HX}}(\Theta_{\text{eng}} - \Theta_{\text{cw}})$.

A.2. Radiator model

Spatially discretised into two segments:

$$C_{\text{rad}}\dot{\Theta}_{\text{rad},1} = (\dot{m}c_p)_{\text{cw}}(\Theta_{\text{cw}} - \Theta_{\text{rad},1}) \tag{A.3}$$
$$C_{\text{rad}}\dot{\Theta}_{\text{rad},2} = (\dot{m}c_p)_{\text{cw}}(\Theta_{\text{rad},1} - \Theta_{\text{rad},2}) - \Phi_{\text{rad}} \tag{A.4}$$

where $\Phi_{\text{rad}} = H^*_{\text{rad}}(\Delta\Theta)^{\kappa}$ and $\Delta\Theta = (\Theta_{\text{rad},1} + \Theta_{\text{rad},2})/2 - \Theta_{\text{a}}$.

A.3. Zone model

Air and structure:

$$C_{\text{a}}\dot{\Theta}_{\text{a}} = H_{\text{s}}(\Theta_{\text{s}} - \Theta_{\text{a}}) + H_{\text{loss}}(\Theta_{\text{e}} - \Theta_{\text{a}}) + \Phi_{\text{rad}} + f_{\text{int,a}}\Phi_{\text{load}} \tag{A.5}$$
$$C_{\text{s}}\dot{\Theta}_{\text{s}} = H_{\text{s}}(\Theta_{\text{a}} - \Theta_{\text{s}}) + f_{\text{int,s}}\Phi_{\text{load}} \tag{A.6}$$

References

[1] E. Entchev, L. Yang, M. Ghorab, E. Lee, Performance analysis of a hybrid renewable microgeneration system in load sharing applications, Appl. Therm. Eng. 71 (2) (2014) 697–704, http://dx.doi.org/10.1016/j.applthermaleng.2013.10.057. <http://www.sciencedirect.com/science/article/pii/S135943111300776X>.

[2] F. Sossan, H. Bindner, H. Madsen, D. Torregrossa, L.R. Chamorro, M. Paolone, A model predictive control strategy for the space heating of a smart building including cogeneration of a fuel cell-electrolyzer system, Int. J. Electr. Power Energy Syst. 62 (2014) 879–889, http://dx.doi.org/10.1016/j.ijepes.2014.05.040. <http://www.sciencedirect.com/science/article/pii/S0142061514003111>.

[3] P. Wolfrum, M. Kautz, J. Schäfer, Optimal control of combined heat and power units under varying thermal loads, Control Eng. Pract. 30 (2014) 105–111, http://dx.doi.org/10.1016/j.conengprac.2013.08.014. <http://www.sciencedirect.com/science/article/pii/S0967066113001603>.

[4] J. Kortela, S.-L. Jämsä-Jounela, Modeling and model predictive control of the BioPower combined heat and power (CHP) plant, Int. J. Electr. Power Energy Syst. 65 (2015) 453–462, http://dx.doi.org/10.1016/j.ijepes.2014.10.043. <http://www.sciencedirect.com/science/article/pii/S0142061514006462>.

[5] M.H. Moradi, M. Hajinazari, S. Jamasb, M. Paripour, An energy management system (EMS) strategy for combined heat and power (CHP) systems based on a hybrid optimization method employing fuzzy programming, Energy 49 (2013) 86–101, http://dx.doi.org/10.1016/j.energy.2012.10.005. <http://www.sciencedirect.com/science/article/pii/S0360544212007670>.

[6] E. Entchev, P. Tzscheutschler, Integration of Microgeneration and Related Technologies in Building Tech. Rep. October, International Energy Agency, Germany, 2014.

[7] I. Staffell, D.J.L. Brett, N.P. Brandon, A.D. Hawkes, Domestic Microgeneration: Renewable and Distributed Energy Technologies, Policies and Economics, Routledge, Abingdon, Oxon, UK, 2015.

[8] J.-J.E. Slotine, W. Li, Applied Nonlinear Control, Prentice Hall, New Jersey, 1991.

[9] D. Cheng, A. Isidori, W. Respondek, T.J. Tarn, Exact linearization of nonlinear systems with outputs, Math. Syst. Theory 21 (1) (1988) 63–83, http://dx.doi.org/10.1007/BF02088007. <http://dx.doi.org/10.1007/BF02088007>.

[10] J. Arif, S. Ray, B. Chaudhuri, MIMO feedback linearization control for power systems, Int. J. Electr. Power Energy Syst. 45 (1) (2013) 87–97, http://dx.doi.org/10.1016/j.ijepes.2012.08.051. <http://www.sciencedirect.com/science/article/pii/S0142061512005017>.

[11] L. Roca, J.L. Guzman, J.E. Normey-Rico, M. Berenguel, L. Yebra, Filtered Smith predictor with feedback linearization and constraints handling applied to a solar collector field, Sol. Energy 85 (5) (2011) 1056–1067, http://dx.doi.org/10.1016/j.solener.2011.02.026. <http://www.sciencedirect.com/science/article/pii/S0038092X1100079X>.

[12] H. Moradi, M. Saffar-Avval, A. Alasty, Nonlinear dynamics, bifurcation and performance analysis of an air-handling unit: disturbance rejection via feedback linearization, Energy Build. 56 (2013) 150–159, http://dx.doi.org/10.1016/j.enbuild.2012.09.017. <http://www.sciencedirect.com/science/article/pii/S0378778812004677>.

[13] A. Isidori, A. Ruberti, On the synthesis of linear input-output responses for nonlinear systems, Syst. Control Lett. 4 (1) (1984) 17–22, http://dx.doi.org/10.1016/S0167-6911(84)80046-8. <http://www.sciencedirect.com/science/article/pii/S0167691184800468>.

[14] A. Isidori, Nonlinear Control Systems, Springer-Verlag, New York, NY, USA, 1989.

[15] C.-F. Lin, Advanced Control Systems Design, Prentice Hall, Englewood Cliffs, NJ, USA, 1994.

[16] R.M. Phelan, Automatic Control Systems, Cornell University Press, London, UK, 1977.

[17] A. Hansson, P. Gruber, J. Tödtli, Fuzzy anti-reset windup for PID controllers, Control Eng. Pract. 2 (3) (1994) 389–396, http://dx.doi.org/10.1016/0967-0661(94)90775-7. <http://www.sciencedirect.com/science/article/pii/0967066194907757>.

[18] U. Arndt, I. Beausoleil-Morrison, M. Davis, W. D'haeseleer, V. Dorer, E. Entchev, A. Ferguson, J. Gusdorf, N. Kelly, M. Manning, L. Peeters, M. Sasso, D. Schreiber, S. Sibilio, K. Siemens, M. Swinton, Experimental Investigation of Residential Cogeneration Devices and Calibration of Annex 42 Models Tech. rep., Annex 42 of the International Energy Agency Energy Conservation in Buildings and Community Systems Programme, 2007.

[19] National Renewable Energy Laboratory, PVWatts, 2012. <http://rredc.nrel.gov/solar/calculators/PVWATTS/version1/>.

[20] G. Conroy, A. Duffy, L. Ayompe, Validated dynamic energy model for a Stirling engine μ-CHP unit using field trial data from a domestic dwelling, Energy Build. 62 (2013) 18–26, http://dx.doi.org/10.1016/j.enbuild.2013.01.022. <http://www.sciencedirect.com/science/article/pii/S0378778813000534>.

[21] H. Lee, J. Bush, Y. Hwang, R. Radermacher, Modeling of micro-CHP (combined heat and power) unit and evaluation of system performance in building application in United States, Energy 58 (2013) 364–375, http://dx.doi.org/10.1016/j.energy.2013.05.015. <http://www.sciencedirect.com/science/article/pii/S036054421300399X>.

[22] J. Godefroy, R. Boukhanouf, S. Riffat, Design, testing and mathematical modelling of a small-scale CHP and cooling system (small CHP-ejector trigeneration), Appl. Therm. Eng. 27 (1) (2007) 68–77, http://dx.doi.org/10.1016/j.applthermaleng.2006.04.029. <http://www.sciencedirect.com/science/article/pii/S135943110600175X>.

[23] I. Beausoleil-Morrison, A. Ferguson, B. Griffith, N. Kelly, F. Maréchal, A. Weber, Specifications for Modelling Fuel Cell and Combustion-Based Residential Cogeneration Devices within Whole-Building Simulation Programs Tech. rep., Annex 42 of the International Energy Agency Energy Conservation in Buildings and Community Systems Programme, 2007, <www.cogen-sim.net>.

[24] A. Rosato, S. Sibilio, Calibration and validation of a model for simulating thermal and electric performance of an internal combustion engine-based micro-cogeneration device, Appl. Therm. Eng. 45–46 (2012) 79–98, http://dx.doi.org/10.1016/j.applthermaleng.2012.04.020. <http://www.sciencedirect.com/science/article/pii/S1359431112002633>.

[25] I. Beausoleil-Morrison, A. Ferguson, Inter-model Comparative Testing and Empirical Validation of Annex 42 Models for Residential Cogeneration Devices Tech. rep., Annex 42 of the International Energy Agency Energy Conservation in Buildings and Community Systems Programme, 2007.

[26] J. Allison, G.B. Murphy, J.M. Counsell, Control of micro-CHP and thermal energy storage for minimising electrical grid utilisation, Int. J. Low-Carbon Technol. 11 (1) (2016) 109–118, http://dx.doi.org/10.1093/ijlct/ctu023. <http://ijlct.oxfordjournals.org/content/early/2014/08/20/ijlct.ctu023.abstract>.

[27] BS EN 15265:2007, Energy Performance of Buildings, Calculation of Energy Needs for Space Heating and Cooling Using Dynamic Methods, General Criteria and Validation Procedures, first ed., British Standards Institution, London, UK, 2007. http://dx.doi.org/10.3403/30136887. <http://https://bsol.bsigroup.com/Bibliographic/BibliographicInfoData/000000000030136887>.

[28] A.P. Ramallo-González, M.E. Eames, D.A. Coley, Lumped parameter models for building thermal modelling: an analytic approach to simplifying complex multi-layered constructions, Energy Build. 60 (2013) 174–184, http://dx.doi.org/10.1016/j.enbuild.2013.01.014. <http://www.sciencedirect.com/science/article/pii/S0378778813000315>.